International Journal of Computer Information Systems and Industrial Management Applications
ISSN 2150-7988 Volume 18 (2026) pp. 1-11

https://doi.org/10.70917/ijcisim-2026-0375
Article

Deep learning-based dynamic monitoring technology for soil moisture in upland turf stripping

Yan Liu [1,2], Ji Wang [1,*] and Ming Zhao [3]

[1] College of Desert Control Science and Engineering, Inner Mongolia Agricultural University, Hohhot, Inner Mongolia, 010018, China
[2] School of Modern Services and Management, Inner Mongolia Technical College of Construction, Hohhot, Inner Mongolia, 010010, China
[3] Hohhot Natural Resources Bureau, Hohhot, Inner Mongolia, 010000, China
* Correspondence author: wangji19572024@126.com

Abstract: In this paper, the inversion of soil moisture in highland turf stripping was carried out by constructing an artificial neural network model, improving the vegetation-adjusted vertical drought index (VAPDI), and processing CYGNSS data. The accuracy of the inversion model was verified by linearly fitting the VAPDI calculated from remote sensing images in the observation area and the measured soil moisture data in the same period in SPSS. More accurate reflectance was obtained by surface roughness attenuation correction. After integrating the topographic feature quantity, the accuracy of the model inversion situation was analyzed by comparing the index situation of the artificial neural network model with other models. The linear regression model for a total of three periods of data from 2020-2022 in the observation area passed the significance test of 0.05. The interpolated Bias, RMSE, and R values of the artificial neural network model were better than those of the other comparative models, and the training time was 30% and 15% less than that of the other models. The model inversion results were consistent with the actual soil moisture situation with high accuracy.

Keywords: soil moisture; VAPDI index; CYGNSS data; artificial neural network; albedo correction; topographic feature volume

1. Introduction

Turf stripping soil moisture dynamic monitoring is an important indicator of soil physicochemical property analysis, which has important significance for environmental protection and soil quality evaluation. Turf stripping soil moisture dynamic monitoring can be used to understand the health status and pollution degree of the soil by detecting various components and their contents in the soil, and provide a scientific basis for soil protection and management [1-2]. Soil moisture is an important parameter describing the soil moisture condition, which is of great significance in the fields of agricultural production, water resource management and earth system science. Traditional soil moisture monitoring methods usually rely on field sampling and laboratory analysis, which are not only time-consuming and labor-intensive, but also difficult to realize large-scale, real-time monitoring [3-4].

In recent years, the development of microwave remote sensing technology provides a new solution for soil moisture monitoring. Microwave remote sensing technology to monitor soil moisture has many advantages, such as microwave signals have a unique sensitivity to water molecules, which can accurately reflect the soil moisture status. At the same time, microwave remote sensing technology is characterized by strong penetration and is not affected by cloud cover and adverse weather conditions, which can realize all-weather and large-scale monitoring [5-8]. However, there are still some

shortcomings in microwave remote sensing technology for monitoring soil moisture, such as the influence of factors such as soil type, ground cover and climatic conditions, as well as the lack of uniform calibration methods and data product standards. Therefore, deep learning-based monitoring techniques are gradually being applied to the dynamic monitoring of soil moisture.

Literature [9] analyzes the current status of large-scale soil moisture monitoring, reveals some key research needs to optimize the use of increasingly available soil moisture data, and highlights improvements in earth system monitoring that can help advance the science and practice of soil moisture monitoring. Literature [10] demonstrated that SMosSWDI can well reproduce soil moisture balance dynamics and is useful for tracking agricultural droughts by calculating the soil water deficit index (SWDI) using the SMOSL2 soil moisture sequence in a region. Literature [11] combined manual and real-time monitoring data to characterize slope soil moisture dynamics with good spatial coverage and temporal resolution, revealing that soil moisture dynamics on slopes can be reliably predicted using both SMLR and SVM. Literature [12] analyzed the RTCSM technology based on a literature review, explored its key barriers, and provided observations that not only bridged the knowledge gap in the implementation of spatio-temporal uninterrupted soil monitoring and soil management, but also emphasized the significance of the application of RTCSM in the agricultural and environmental fields. Literature [13] provides an overview of sandy SM monitoring under the driest conditions observed in a study area and emphasizes that SM measurement models are potentially valuable tools for planning sustainable agriculture, especially in countries frequently affected by drought. Literature [14] describes the Swiss soil moisture monitoring network SOMOMOUNT, develops a description of its instrumentation and calibration procedures, and discusses the soil type, climate dependence and its altitudinal distribution of the liquid soil moisture data collected by the project. Literature [15] monitored and analyzed volumetric soil moisture content in bare ground agricultural fields, illustrating the need for continuous soil moisture monitoring in order to support decision making for planning effective irrigation water management and to avoid yield loss of crops during their growth phase as well as quality degradation due to water stress. Literature [16] emphasized the importance of soil moisture by proposing a method for obtaining surface soil moisture (SSM) from the S-1 satellite, highlighting the method's ability to capture soil moisture changes well. Literature [17] conducted a study in a mature “Hass” avocado orchard in central Chile, revealing that the establishment of effective criteria for irrigation governance is a key point and that a baseline of stress-free trees can achieve better water savings. Literature [18] evaluated the ability of DPHP sensors to measure changes in near-surface water content in order to understand the impact of water content on carbon exchange, revealing that there are significant differences between sensor technologies, and that sensitive data from shallow installations can be utilized to estimate the potential for carbon exchange in the biotic enclosure. Literature [19] explores the multifaceted areas of satellite-based soil moisture monitoring, particularly in terms of application party sensitivity, technological advances, and impacts on agriculture and ecosystems, with the aim of optimizing agricultural practices and thus protecting ecosystems.

In this paper, based on different methods of differentiating soil moisture, a more appropriate relative soil moisture content is chosen as the research standard. In order to improve the inversion accuracy of soil moisture in vegetation-covered areas, the vegetation-adjusted vertical drought index is chosen to overcome the influence of other factors. An artificial neural network model was constructed based on the processed CYGNSS data. The data from the observation network were used to analyze the linear correlation between the VAPDI calculated from remote sensing images and the measured soil moisture data in the same period. After correcting the reflectance, three topographic feature quantities, elevation, slope direction and surface roughness, were added to the CYGNSS parameters to obtain the optimized artificial neural network model. The inversion performance and operation efficiency of the model are compared with the other 2 inversion models in terms of indicator values and training time. The artificial neural network model was applied to the soil moisture inversion in the observation area, and the accuracy of the model inversion was judged by comparing the inversion results with the actual soil moisture.

2. Analysis of soil moisture-related concepts and inversion methods

This section analyzes the concepts related to soil moisture and explicitly chooses to use relative soil moisture content to express soil moisture. The limitations of the vertical drought index (PDI) are analyzed, and the improved vertical drought index (MPDI) and vegetation-adjusted vertical drought index (VAPDI) are introduced in a targeted manner. CYGNSS data were processed to construct an artificial neural network model (ANN) for inversion of soil moisture for upland turf stripping.

2.1. Soil moisture and aridity index

2.1.1. Analysis of soil moisture content

Soil moisture, also known as soil moisture, soil water content, soil water content, indicates the water in the soil surface layer that can be absorbed and utilized by plants, and is mainly used to illustrate the water content and water-holding capacity of the soil. Soil moisture can be expressed by soil weight water content, soil volume water content, soil effective water content, soil volumetric water content, soil water storage and soil water potential, etc., while soil relative water content, soil weight water content and soil volumetric water content are more commonly used in the remote sensing inversion of soil moisture.

Soil weight water content, also known as absolute soil water content, that is, the ratio of soil moisture to the weight of the corresponding soil dry soil, expressed as a percentage of weight, which is a classic method of soil water content, with high precision, but the determination and calculation process is complicated, time-consuming and labor-intensive; soil volumetric water content represents the ratio of the volume of water in the soil to the total volume of the soil, which indicates that the water fills up the soil pore space, expressed as a percentage of volume. Soil volumetric water content is the ratio of the volume of water in the soil to the total volume of the soil, which indicates the degree of water filling the soil pores, expressed as a percentage by volume, and the soil volumetric water content and weight water content can be directly converted by the corresponding formula; soil relative water content is often referred to as the soil relative humidity, which refers to the percentage of the weight water content of the soil to the water holding capacity of the field, which indicates the water content in the surface soil that is sufficient to be absorbed and evaporated by vegetation, and it can be used to quantitatively assess the soil humidity status of a certain time range. Relative soil moisture content can reflect most of the information of soil moisture status and surface hydrological processes, and can accurately reflect the drought conditions in agriculture, according to the relative soil moisture content can understand the degree of soil water holding at a certain time, which is an important reference value in irrigation, so this paper chooses to use the relative soil moisture content to express soil moisture.

2.1.2. Improved vertical drought indices

The vertical drought index does not take into account the strong scattering effect of surface vegetation cover on red and near-infrared bands, so it is mainly applicable to remote sensing inversion of soil moisture in areas with low vegetation cover or bare soil, and the inversion accuracy is less satisfactory for regions with large differences in the types of surface cover. To address this limitation, in order to improve the application range of the model, Abdulwasti et al. introduced the vegetation cover degree fv to decompose the mixed pixels of medium remote sensing images in the two-dimensional spectral eigenspace, overcoming the scattering effect of vegetation on the red and near-infrared wavelengths, and acquiring the pure soil pixel reflectance related to soil moisture, and obtaining an improved vertical aridity index:

$$MPDI = \frac{R_{red} + M \cdot R_{nir} - f_v \left(R_{red,v} + M \cdot R_{nir,v} \right)}{\left(1 - f_v \right) \sqrt{M^2 + 1}} \tag{1}$$

where $R_{red,v}$ and $R_{nir,v}$ are the reflectance of vegetation in the red and near-infrared bands, and M is the slope of the soil line; vegetation cover fv can be calculated using the image element dichotomous modeling method:

$$f_v = \left(\frac{NDVI - NDVI_S}{NDVI_V - NDI_S} \right)^2 \tag{2}$$

where $NDVI_v$ and $NDVI_s$ represent the normalized vegetation index (NVI) for vegetated and bare soil in the study area, respectively.

In the Nir-Red two-dimensional spectral feature space, the direction perpendicular to the soil line indicates the variation of vegetation cover with MPDI, and the direction parallel to the soil line indicates the variation of soil moisture with MPDI, and the decrease of both soil moisture and vegetation cover increases the value of MPDI and vice versa.

2.1.3. Vegetation-adjusted vertical aridity index (VAI)

In order to further analyze the effect of mixed pixels in Nir-Red spectral feature space on the spectral information of soil moisture and to improve the inversion accuracy of soil moisture in the

vegetation cover area, after analyzing the error distribution law of the PDI model, the vertical vegetation index (PVI) was introduced to characterize the vegetation cover information of different pixels, and the PDI model was adjusted in the two-dimensional space of PVI-PDI, and the vegetation-adjusted vertical drought index (PDI) was proposed to be suitable for remote sensing inversion of soil moisture in the high-vegetation cover area. The PDI model was adjusted in the two-dimensional space of PVI-PDI, and the vegetation-adjusted vertical drought index was proposed to be suitable for remote sensing inversion of soil moisture in high vegetation cover areas.

Figure 1 shows the scatter distribution of the spatial image elements of the PVI-PDI spectral features. All the contours of soil moisture in triangle ABC are approximated as straight lines, and each contour intersects at point A. In the bare soil area of $PVI = 0$, it is more accurate to estimate soil moisture by PDI, so the PDI of any point E in ABC can be replaced by the PDI of the intersection of the soil moisture contour AE and the transverse coordinate axis at point F, in which the length of OF can be taken as the corrected PDI of point E. Based on the principle of similarity of the triangles According to the principle of triangle similarity, the formula of VAPDI at any X points can be obtained:

$$VAPDI(X) = PDI(A) - \frac{|PDI(A) - PDI(X)| * PVI(A)}{PVI(A) - PVI(X)} \tag{3}$$

In the formula, the vertical vegetation index PVI is calculated as follows:

$$PVI = \frac{\left|R_{nir} - M \cdot R_{red} - I\right|}{\sqrt{M^2 + 1}} \tag{4}$$

Theoretically, VAPDI is equal to PDI for bare soil areas i.e. when PVI tends to zero.

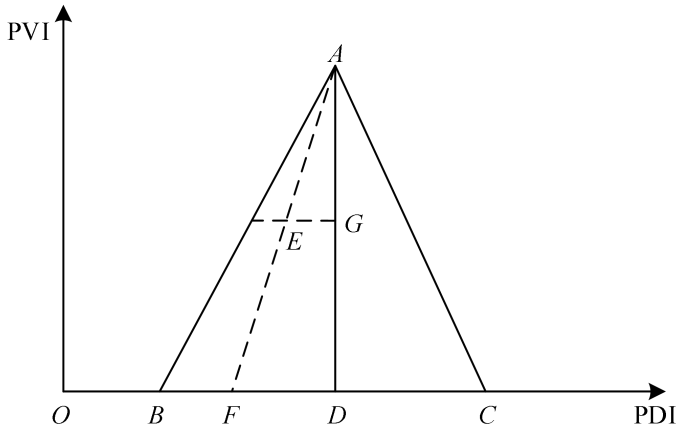

Figure 1. PVI-PDI spectral feature space pixel scatter distribution diagram

2.2. Inversion methods

2.2.1. CYGNSS data

The CYGNSS constellation consists of eight satellites distributed in near-Earth orbits at an altitude of about 509km, with satellite orbital inclination of about 34.5°, and its detection range is between 38.5°S and 38.5°N, which covers the entire study area of this paper.CYGNSS utilizes the on-board GNSS-R receivers to receive the GNSS reflection signals from the ground and generate delayed-Doppler maps (DDMs) by code correlation with received GNSS direct signals.DDM is the basic observation quantity of GNSS-R, which contains physical information of the reflected surface as L1 of CYGNSS. code correlation with the received GNSS direct signals to generate delay-Doppler maps (DDMs).DDMs are the basic observables of GNSS-R, which contain the physical information of the reflecting surfaces, and are publicly released on the official website of CYGNSS as a CYGNSS level L1 product with a time delay of 3-6 d. Table 1 shows the main parameters of the CYGNSS level L1 version 2.1 product. In this paper, the CYGNSSL1 level 2.1 version of the product is used for the time period from January 1, 2020 to December 31, 2022.

Table 1. Key variables of CYGNSS level 1 products(version 2.1)

Variable symbol	Variable name	Unit	Instructions
P	Power-analog	Watt	DDM power
P^t	Gps-tx-power-db-w	DB	GPS signal transmission power
R_{st}	Rx-to-sp-range	M	Distance from the CYGNSS satellite to the specular reflection point
R_{ts}	Tx-to-sp-range	M	Distance from GPS satellite to specular reflection point
G^t	Gps-ant-gain-db-i	DBi	GPS signal transmitting antenna gain
G^r	Sp-rx-gain	DBi	CYGNSS reflected signal receiving antenna gain
B	Sp-lat	Degree	Latitude of specular reflection point
L	Sp-lon	Degree	Longitude of specular reflection point
θ	Sp-inc-angle	Degree	Angle of incidence of specular reflection point

2.2.2. CYGNSS data processing

CYGNSSL Level 1 products require further calculations to generate surface reflectance before they can be used for soil moisture inversion. Prior to computation, quality control of the DDM is required to reject data with reflected signal incidence angles greater than 65° or receiver antenna gains less than 0. Then, the expression for the energy maximum P_r in the DDM is extracted, assuming that P_r comes mainly from surface coherent scattering:

$$P_r = \frac{P^t G^t}{4\pi\left(R_{ts}+R_s\right)^2}\frac{G^r\lambda^2}{4\pi}\Gamma_s(\theta) \tag{5}$$

The right parameter λ in Eq. (5) is the GPSL1 signal wavelength (19 cm), Γ_s is the surface reflectance, and the other parameters are provided by CYGNSS L1 products (Table 1). The surface reflectance in Eq. (5) is converted to db units:

$$\begin{aligned}\Gamma_s(\theta) = {} & 10\log_{10}\left(P_r\right)-10\log_{10}\left(P^tG^t\right)\\ & -10\log_{10}\left(G^r\right)-20\log_{10}(\lambda)+20\log_{10}\left(R_{ts}+R_s\right)\\ & +20\log_{10}(4\pi)\end{aligned} \tag{6}$$

Processing the quality-controlled DDM according to Eqs. (5) and (6) yields the surface reflectance of the corresponding reflection point, or more precisely, the surface reflectance of the Fresnel reflection zone in which the surface reflection point is located, whose coverage is determined by the scattering characteristics: in the case of coherent scattering, the coverage is 0.5km × 7km; in the case of incoherent scattering, the coverage increases rapidly to The surface reflectance is affected by the angle of incidence and can be corrected using equation (7):

$$\Gamma_s = \Gamma_s(\theta)-10\log_{10}\cos^n(\theta) \tag{7}$$

In Eq. (7), n is a constant between [0,2], and $n=1.5$ is taken in this paper.

Surface reflectance has a strong relationship with surface dielectric constant, and the latter is mainly determined by soil moisture, thus establishing the connection between surface reflectance and soil moisture, which is the theoretical basis for GNSS-R inversion of soil moisture. The relationship between surface reflectance and soil moisture is complex, and empirical fitting is generally used to establish the GNSS-R inversion surface soil moisture model. For the subsequent neural network inversion of soil moisture, it is necessary to match the CYGNSS surface reflectance gridded with the 37km × 37km EASE grid used by the SMAP satellite. In this paper, all the reflectance values falling within the grid each day are averaged as the surface reflectance for that grid. After processing, we found that areas with higher soil moisture also have higher surface reflectance.

2.2.3. Artificial neural network models

The relationship between surface albedo and surface soil moisture is nonlinear and is strongly influenced by environmental change factors (vegetation cover and surface roughness, etc.). Therefore, in order to obtain more accurate surface soil moisture by inversion, it is necessary to model the

relationship between soil moisture and surface reflectance and environmental factors. However, surface reflectance and soil moisture as well as the complex connections between the parameters make it extremely difficult to establish a physical model, therefore, this paper adopts an artificial neural network approach for GNSS-R soil moisture inversion, which is data-driven and can well model the complex nonlinear relationships between the parameters.

A typical artificial neural network consists of input, hidden and output layers. Before training the neural network model, we first need to determine the input layer parameters, in addition to the CYGNSS surface reflectance, and the three parameters provided by the SMAP satellite, namely, normalized vegetation index (NDVI), surface roughness, and feature type, considering the spatial and temporal variations of the soil moisture at the surface, we can subsequently introduce the three-dimensional coordinates (latitude, longitude, latitude, and elevation H) and the yearly cumulative days (DOY) as input parameters. DOY as input parameters. Considering consistency and reliability, we chose SMAP soil moisture as the target parameter for training the artificial neural network inversion. For the selection of the number of hidden layers and nodes of the artificial neural network model, we determined that the number of hidden layers of the artificial neural network model used in this paper is 3, and each layer contains 35 nodes after several experiments, taking into account the fitting accuracy and model complexity.

3. Artificial neural network model optimization and application

In this part, the correlation between the VAPDI calculated from remote sensing images in the selected observation area and the measured soil moisture data during the same period is analyzed by linear fitting in SPSS. The corrected reflectance is obtained after surface roughness attenuation correction. On this basis, three topographic features, namely elevation, slope direction and surface roughness, were added to the CYGNSS parameters to obtain the optimized artificial neural network model. The inversion effect of this model is compared with other models, and the difference between the inversion results of this model and the actual soil moisture condition.

3.1. Upland turf stripping soil moisture observation network data

The Plateau Turf Stripping Soil Temperature and Moisture Observation Network (longitude: 91.5°E-92.5°E, latitude: 31°N-32N) is located in a spatial area of 101 km × 101 km in the semi-humid zone of the central Tibetan Plateau, with an average elevation of 4655 m. The topography of the deployment area of the network is flat and at the same time has low biomass, which makes it an ideal area for evaluating the inversion of soil moisture from satellites. The network was deployed with 51 observation sites, and at each site a sensor was tilted to insert 0.1-5.5 cm into the topsoil, which is comparable to the penetration depth of the L -band passive microwave sensors CYGNSS and SMAP, with a measurement interval of 35 min. The network provided soil moisture data at three spatial scales: 1.1° × 1.1° (corresponding to GCM grid scale), 0.35° × 0.1°, and 0.35° × 0.1° (corresponding to the GCM grid scale). , 0.35°×0.35° (corresponding to the passive microwave satellite pixel scale), and 0.15°×0.15° (corresponding to the active-passive fusion microwave pixel scale). In this paper, the measured data with an observation depth of 5.5 cm and a spatial observation scale of 0.35°×0.35° are selected for the construction of the inversion model. In the process of collecting data to construct the model, due to the complexity of the actual observation environment, the reflectivity will be affected by the environment and deviate from the real value, so it needs to be corrected. In this paper, the reflectance is corrected for the attenuation of the signal by the surface roughness.

3.2. Fitting results of artificial neural network model based on VAPDI

In order to meet the need for accuracy verification of the inversion model, before constructing the artificial neural network model based on VAPDI for the turf stripping area in the network deployment area, it is necessary to divide the sampling points of soil moisture measured data in the area. Two thirds of the soil moisture sampling points are used for constructing the inversion model, and one third is used for verification and evaluation of the accuracy of the inversion model. A total of 51 samples were sampled in each phase of the turf stripping area, and the same point was sampled once each in 2020, 2021 and 2022, respectively, of which 34 were selected as the modeling sample set, and the remaining 17 sample points were used as the validation sample set for inversion model accuracy validation and evaluation.

Figures 2, 3, and 4 show the fitting results of the VAPDI-based artificial neural network model for the turf stripping area in 2020, 2021, and 2022, respectively. The artificial neural network model of the sod-stripping region for a total of three periods of remote sensing imagery was obtained by linear fitting analysis in SPSS between the VAPDI calculated from the remote sensing imagery of the

sod-stripping region for a total of three periods and the measured soil moisture data for the same period.

As can be seen from the results of the univariate linear regression analysis between the VAPDI of each period of remote sensing images and the measured soil moisture data in Figures 2-Figure 4, all the regression models of the VAPDI soil moisture regression model of the turf stripping region for a total of three periods of remote sensing images passed the significance test of 0.05, which indicates that the three regression models are statistically significant, and that the VAPDI value of each period of remote sensing images and its corresponding soil moisture data can be seen to be statistically significant. VAPDI value and its corresponding soil moisture have different degrees of linear correlation.

By combining the mean value of vegetation cover with the regression model, it can be found that when the mean value of vegetation cover is 0.358642, the coefficient of determination of the inverse model for this period is the highest at 0.5724, and at the same time, with the increase of vegetation cover, the coefficient of determination of the model decreases, and the coefficient of determination of the inverse model for this period is the lowest at 0.499 of all the models when the maximum value of vegetation cover is 0.675651. The ANN inversion model based on the VAPDI index to invert the soil moisture in the sod-stripped area tended to weaken with the increase of the vegetation cover in the sod-stripped area, which indicated that the VAPDI had a better inversion of soil moisture in the low-vegetation area, and that the inversion effect of the ANN inversion model deteriorated with the increase of the vegetation cover.

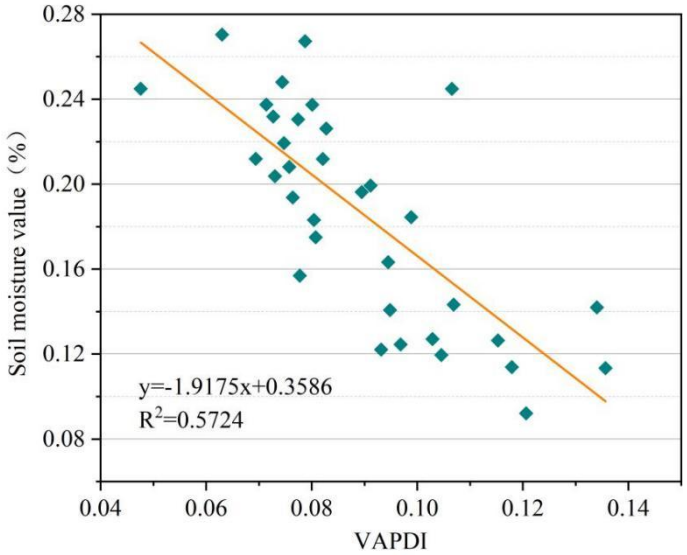

Figure 2. Regression analysis of image VAPDI and soil water data in 2020

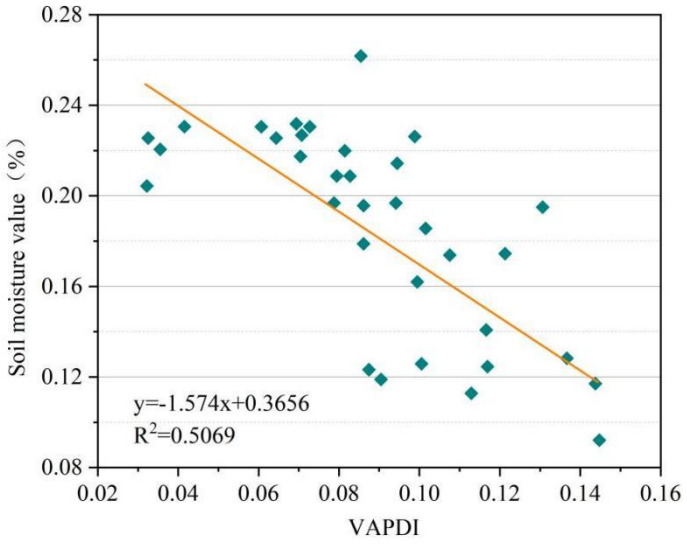

Figure 3. Regression analysis of image VAPDI and soil water data in 2021

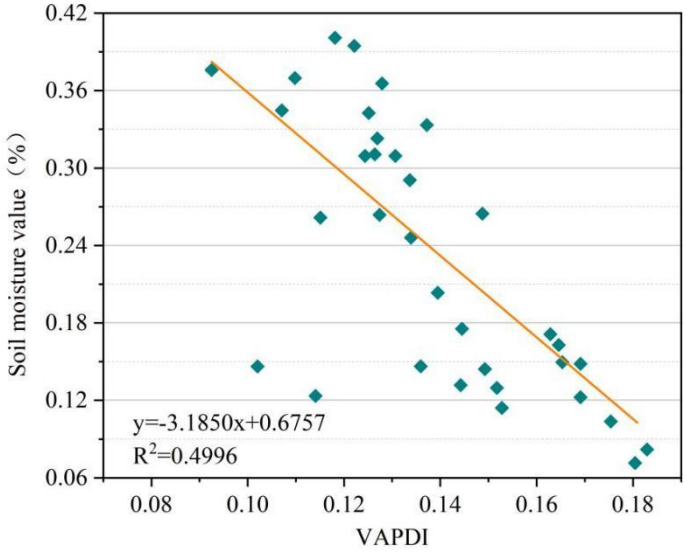

Figure 4. Regression analysis of image VAPDI and soil water data in 2022

3.3. Surface roughness attenuation correction

Surface roughness is one of the characteristic quantities of environmental factors that affect the power of interest. Its causing attenuation can be expressed as:

$$S_r = 4k^2h^2\cos\theta \tag{8}$$

k is the wave number $(2\pi/\lambda)$; h is the surface roughness provided by SMAP; and θ is the angle of incidence provided by CYGNSS.

The reflectivity corrected for surface roughness attenuation is:

$$\Gamma_3 = \Gamma_2 \times \exp(S_r) \tag{9}$$

Γ_3 is the reflectance after roughness correction, which is the parameter used to build the machine learning model. Fig. 5 is the comparison graph before and after correction of random 480 reflectance on August 3, 2021, from Fig. 5, it can be seen that the change of reflectance before and after correction is more obvious, which proves that the correction of reflectance is necessary.

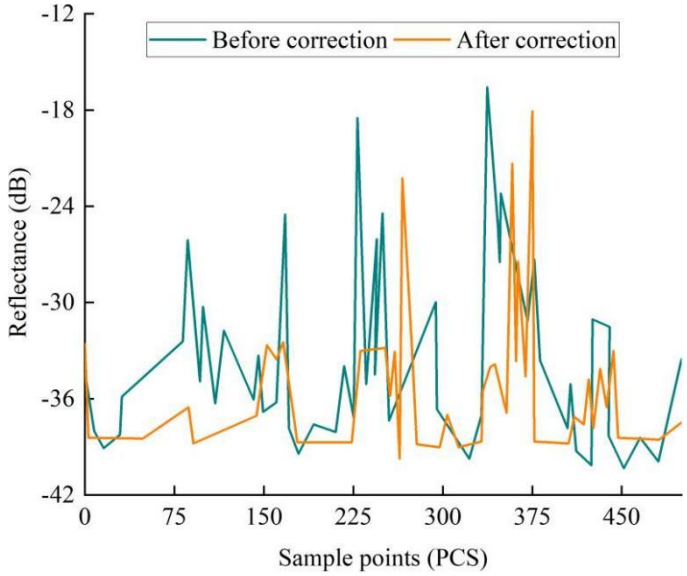

Figure 5. Comparison of reflectance before and after correction

3.4. Comparison of fused terrain feature volume models

The artificial neural network model, RF inversion model, and SVR inversion model were constructed based on the CYGNSS parameters (corrected reflectance Γ_3) by adding only three topographic feature quantities (elevation, slope direction, and surface roughness), using the data from the turf stripping area in 2021 (75% training set, 25% validation set), respectively. Table 2 shows the inversion results of the artificial neural network model, RF inversion model, and SVR inversion model. From Table 2, it can be seen that the interpolated Bias of the artificial neural network model is -0.0006cm³/cm³, the RMSE is 0.029cm³/cm³, and the R is 0.8613. The results of the artificial neural network model constructed in this paper are better than the RF inversion model and the SVR inversion model in all the three measurements, which indicates that the artificial neural network model has a better inversion performance.

In addition, this paper also conducted experiments comparing the time spent on the less-parameter model (artificial neural network model) and the multi-parameter model (SVR inversion model) using data from this study area. In the model training part, the training time of the less-parameter artificial neural network model in this paper was reduced by 30% compared to the multi-parameter SVR inversion model. In the artificial neural network model extrapolation part, the training time of the less-parameter artificial neural network model in this paper is reduced by 15% compared with the multi-parameter SVR model. Both in the model training part and the model extrapolation part, the operation efficiency of the less-parameter artificial neural network model proposed in this paper is improved.

Table 2. Comparison of inversion results of ANN, RF and SVR

Model	CYGNSS Characteristic quantity	Fusion characteristic quantity	Bias cm³/cm³	RMSE cm³/cm³	R
ANN	Corrected reflectance and incidence Angle	Elevation, slope, surface roughness	**-0.0006**	**0.039**	**0.8613**
RF	Corrected reflectance and incidence Angle	Elevation, slope, surface roughness	-0.0010	0.0585	0.7516
SVR	Reflectance, longitude, latitude, time	Surface roughness, NDVI, elevation, type of surface object	0.011	0.0453	0.856

An artificial neural network model built using CYGNSS (corrected reflectance Γ_3) fused with topographic feature quantities was used to invert the soil moisture conditions in the sod stripping area in 2021. Figure 6 shows the results of the inversion of soil moisture quantities in the turf stripping area in 2021. Most of the true soil moisture in the region is between 0.06 and 0.35 cm³/cm³, with a short period of time when the soil moisture is above 0.35 cm³/cm³. Comparing the real soil moisture situation in the region with the inversion results of the artificial neural network model, it can be clearly seen that the model is able to obtain soil moisture with high precision and high inversion accuracy, and can be used in the dynamic supervision of the soil moisture of the plateau turf stripping over a wide range of long time series.

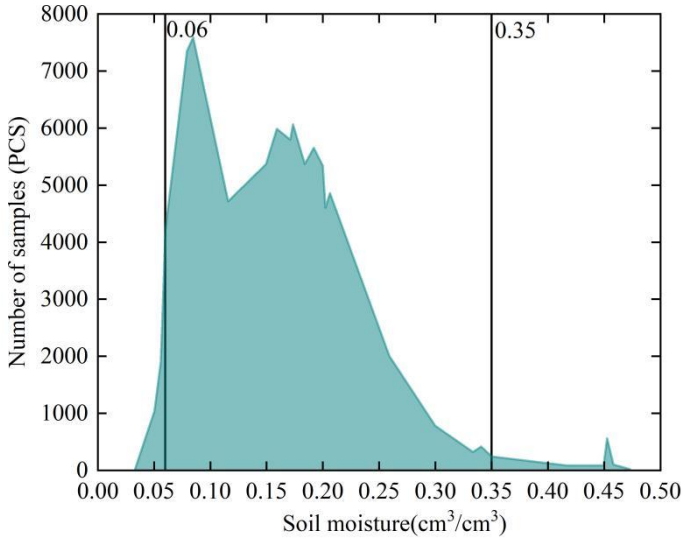

Figure 6. Inversion results of soil moisture quantity in the Khanma burn site in 2021

4. Conclusion

In this paper, a deep learning-based artificial neural network model was constructed and optimized for application in the inversion of soil moisture in highland turf stripping. Linear regression analysis of remote sensing image VAPDI and soil moisture measured data using data from sampling sites from 2020 to 2022 found that the P value of the three periods of data is less than 0.05, which is significant. It indicates that the vegetation cover has a certain effect on the inversion effect of the artificial neural network model. The artificial neural network model in this paper has high accuracy in the inversion of soil moisture in the stripped soil of plateau turf, but in the area with high vegetation cover, the relevant parameters of the model should be adjusted or other inversion models should be selected for the inversion to ensure the accuracy of the inversion.

After the correction of surface roughness attenuation, the reflectance is much different from the original reflectance, which proves that the original reflectance is affected by other factors on the surface, and there may be a certain error situation. Combined with the corrected reflectance, the artificial neural network model is more accurate by integrating the three topographic features of elevation, slope direction and surface roughness in the CYGNSS parameters. Comparing the index values of the three models, the artificial neural network model has an interpolated Bias of -0.0006cm³/cm³, an RMSE of 0.029cm³/cm³, and an R of 0.8613, which are all better than the other models, and the training time is reduced by 30% and 15% in the training part and the extrapolation part. The inversion performance is stronger and runs more efficiently. The inversion results of the observed area of the artificial neural network model show that the soil moisture in the area is mainly between 0.06 and 0.35 cm³/cm³, and with 0.35 cm³/cm³ as the cut-off point, and less than that moisture level is exceeded. The inversion results are consistent with the actual situation, which verifies the inversion accuracy of the artificial neural network model.

Comprehensively, the advantage of the artificial neural network model in this paper is that it can continuously optimize the main parameters to achieve accurate inversion with high operational efficiency. This is highly relevant in the application of dynamic monitoring of soil moisture in highland turf stripping, and is an inversion model worthy of in-depth study.

References

1. Camporese, M., Gumiere, S. J., Putti, M., & Botter, G. (2021). Efficient irrigation of maize through soil moisture monitoring and modeling. Frontiers in Water, 3, 627551.
2. Peng, J., & Loew, A. (2017). Recent advances in soil moisture estimation from remote sensing. Water, 9(7), 530.
3. Mohanty, B. P., Cosh, M. H., Lakshmi, V., & Montzka, C. (2017). Soil moisture remote sensing: State-of-the-science. Vadose Zone Journal, 16(1), 1-9.
4. McColl, K. A., Alemohammad, S. H., Akbar, R., Konings, A. G., Yueh, S., & Entekhabi, D. (2017). The global distribution and dynamics of surface soil moisture. Nature Geoscience, 10(2), 100-104.
5. Yu, L., Gao, W., Shamshiri, R. R., Tao, S., Ren, Y., Zhang, Y., & Su, G. (2021). Review of research progress on soil moisture sensor technology. International Journal of Agricultural and Biological Engineering, 14(4), 32-42.
6. Zhu, L., Suomalainen, J., Liu, J., Hyyppä, J., Kaartinen, H., & Haggren, H. (2018). A review: Remote sensing sensors. Multi-purposeful application of geospatial data, 19.
7. Varotsos, C. A., & Krapivin, V. F. (2020). Microwave remote sensing tools in environmental science. New York, NY, USA: Springer International Publishing.
8. Blackwell, W. J. (2017, June). Technology development for small satellite microwave atmospheric remote sensing. In 2017 IEEE MTT-S International Microwave Symposium (IMS) (pp. 222-225). IEEE.
9. Ochsner, T. E., Cosh, M. H., Cuenca, R. H., Dorigo, W. A., Draper, C. S., Hagimoto, Y., ... & Zreda, M. (2013). State of the art in large-scale soil moisture monitoring. Soil Science Society of America Journal, 77(6), 1888-1919.

10. Martínez-Fernández, J., González-Zamora, A., Sánchez, N., Gumuzzio, A., & Herrero-Jiménez, C. M. (2016). Satellite soil moisture for agricultural drought monitoring: Assessment of the SMOS derived Soil Water Deficit Index. Remote Sensing of Environment, 177, 277-286.
11. Zhu, Q., Zhou, Z., Duncan, E. W., Lv, L., Liao, K., & Feng, H. (2017). Integrating real-time and manual monitored data to predict hillslope soil moisture dynamics with high spatio-temporal resolution using linear and non-linear models. Journal of Hydrology, 545, 1-11.
12. Fan, Y., Wang, X., Funk, T., Rashid, I., Herman, B., Bompoti, N., ... & Li, B. (2022). A critical review for real-time continuous soil monitoring: Advantages, challenges, and perspectives. Environmental Science & Technology, 56(19), 13546-13564.
13. Ha, M. C., Darrozes, J., Llubes, M., Grippa, M., Ramillien, G., Frappart, F., ... & Vu, P. L. (2023). GNSS-R monitoring of soil moisture dynamics in areas of severe drought: example of Dahra in the Sahelian climatic zone (Senegal). European Journal of Remote Sensing, 56(1), 2156931.
14. Pellet, C., & Hauck, C. (2017). Monitoring soil moisture from middle to high elevation in Switzerland: set-up and first results from the SOMOMOUNT network. Hydrology and Earth System Sciences, 21(6), 3199-3220.
15. Kassaye, K. T., Boulange, J., Saito, H., & Watanabe, H. (2020). Monitoring soil water content for decision supporting in agricultural water management based on critical threshold values adopted for Andosol in the temperate monsoon climate. Agricultural Water Management, 229, 105930.
16. Bauer-Marschallinger, B., Freeman, V., Cao, S., Paulik, C., Schaufler, S., Stachl, T., ... & Wagner, W. (2018). Toward global soil moisture monitoring with Sentinel-1: Harnessing assets and overcoming obstacles. IEEE Transactions on Geoscience and Remote Sensing, 57(1), 520-539.
17. Beyá-Marshall, V., Arcos, E., Seguel, Ó., Galleguillos, M., & Kremer, C. (2022). Optimal irrigation management for avocado (cv.'Hass') trees by monitoring soil water content and plant water status. Agricultural Water Management, 271, 107794.
18. Young, M. H., Fenstermaker, L. F., & Belnap, J. (2017). Monitoring water content dynamics of biological soil crusts. Journal of Arid Environments, 142, 41-49.
19. Sabadash, V., & Lopushansky, O. (2023, October). Satellite Monitoring of Soil Moisture: Applications, Technologies and Impact on Agriculture and Ecosystems. In International Conference of Young Professionals «GeoTerrace-2023» (Vol. 2023, No. 1, pp. 1-5). European Association of Geoscientists & Engineers.